



Optimal design of PEM fuel cells to generate maximum power: A CFD study

Maher A.R. Sadiq Al-Baghdadi

Fuel Cell Research Center, International Energy & Environment Foundation, Al-Najaf, P.O.Box 39, Iraq.

Abstract

A full three-dimensional, multi-phase computational fluid dynamics model of a PEM fuel cell has been developed. The parametric study using this model has been performed and discussed in detail. Optimization study of a PEM fuel cell performance has been performed. The study quantifies and analyses the impact of operating, design, and material parameters on fuel cell performance and get an optimal design for PEM fuel cells to generate maximum power. To generate maximum power, the results show that the cell must be operate at higher cell operating temperature, higher cell operating pressure, higher stoichiometric flow ratio, and must have higher GDL porosity, higher GDL thermal conductivity, narrower gases channels, and thinner membrane. At these optimum conditions, the result shows that the total displacement and the degree of the deformation inside the MEA were decreased. However, the Miss stress in the membrane was increased due to higher cell operating temperature.

Copyright © 2011 International Energy and Environment Foundation - All rights reserved.

Keywords: PEM, Durability, Hygro-thermal stress, CFD, Modelling.

1. Introduction

The performance of PEM fuel cells is known to be influenced by many parameters, such as operating temperature, pressure, stoichiometric flow ratio, gas channels width, GDL thickness, membrane thickness, GDL porosity, and GDL thermal conductivity. In order to improve fuel cell performances, it is essential to understand these parametric effects on fuel cell operations. Changing the cell operating parameters can have either a beneficial or a detrimental impact on fuel cell performance. The difficult experimental environment of fuel cell systems has stimulated efforts to develop model that could simulate and predict multi-dimensional coupled transport of reactants, heat and charged species using computational fluid dynamic (CFD) methods. The strength of the CFD numerical approach is in providing detailed insight into the various transport mechanisms and their interaction, and in the possibility of performing parameters sensitivity analyses [1, 2]. The development of physically representative models that allow reliable simulation of the processes under realistic conditions is essential to the development and optimization of fuel cells, the introduction of cheaper materials and fabrication techniques, and the design and development of novel architectures [3-6]. Comprehensive models rely on the determination of a large number of properties and operating parameters and can be much more computationally intensive, leading to longer solution times. However, these disadvantages are typically outweighed by the benefit of being able to assess the influence of a greater number of design parameters and their associated physical processes [7-11]. In this paper, parametric study using this model has been performed and discussed in detail. The study quantifies and analyses the impact of

operating, design, and material parameters on fuel cell performance and get an optimal design for PEM fuel cells to generate maximum power. The analysis helped identifying critical parameters and shed insight into the physical mechanisms leading to a fuel cell performance under various operating conditions.

2. Model description

The three-dimensional CFD model of a PEM fuel cell that used with the stress model was developed and discussed in detail by the current author in his previous paper [2]. In brief, the model is based on the computational fluid dynamics method and considers multi-phase, multi-component flow inside the gas flow channels and the porous media of a PEM fuel cell with straight flow channels. The full computational domain consists of cathode and anode gas flow channels, and the membrane electrode assembly as shown in Figure 1.

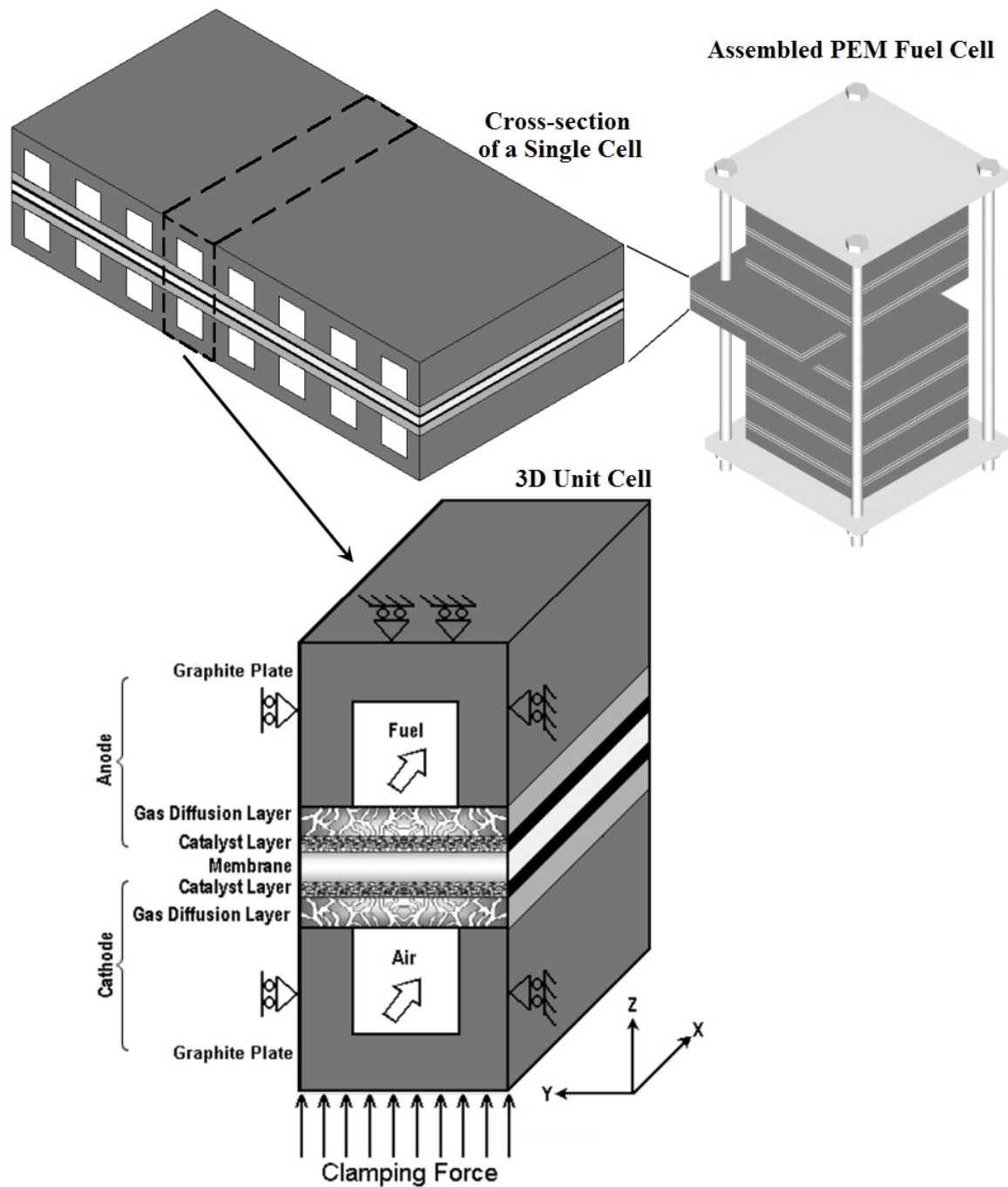


Figure 1. Three-dimensional computational domain

The model accounts for both gas and liquid phase in the same computational domain, and thus allows for the implementation of phase change inside the gas diffusion layers. The model includes the transport of gaseous species, liquid water, protons, energy, and water dissolved in the ion-conducting polymer. Water transport inside the porous gas diffusion layer and catalyst layer is described by two physical mechanisms: viscous drag and capillary pressure forces, and is described by advection within the gas channels. Water transport across the membrane is also described by two physical mechanisms: electro-osmotic drag and diffusion. Water is assumed to be exchanged among three phases; liquid, vapour, and dissolved, and equilibrium among these phases is assumed. This model takes into account convection and diffusion of different species in the channels as well as in the porous gas diffusion layer, heat transfer in the solids as well as in the gases, and electrochemical reactions. A unique feature of the model is to incorporate the effect of hygro-thermal stresses into actual three-dimensional fuel cell model. Numerical techniques, boundary conditions, and procedure algorithm were discussed in detail. A rigorous validation method was used to show good agreement between model predicted results and the experimental data. The model reflects the influence of the operating parameters on fuel cell performance to investigate the in situ total displacement and degree of the deformation of the polymer membrane of PEM fuel cells. The model is shown to be able to understand the many interacting, complex electrochemical, and transport phenomena that cannot be studied experimentally.

3. Results and discussion

The geometric and the base case operating conditions are listed in Table 1. Values of the electrode and membrane parameters for the base case operating conditions are taken from reference [2] and are listed in Table 2.

Table 1. Geometrical and operational parameters for base case conditions

Parameter	Symbol	Value	Unit
Channel length	L	0.05	m
Channel width	W	1e-3	m
Channel height	H	1e-3	m
Land area width	W_{land}	1e-3	m
Gas diffusion layer thickness	δ_{GDL}	0.26e-3	m
Wet membrane thickness (Nafion® 117)	δ_{mem}	0.23e-3	m
Catalyst layer thickness	δ_{CL}	0.0287e-3	m
Hydrogen reference mole fraction	$x_{H_2}^{ref}$	0.84639	-
Oxygen reference mole fraction	$x_{O_2}^{ref}$	0.17774	-
Anode pressure	P_a	3	atm
Cathode pressure	P_c	3	atm
Inlet fuel and air temperature	T_{cell}	353.15	K
Relative humidity of inlet fuel and air (fully humidified conditions)	ψ	100	%
Air stoichiometric flow ratio	ξ_c	2	-
Fuel stoichiometric flow ratio	ξ_a	2	-

3.1 Base case operating conditions

The Membrane-Electrode-Assembly (MEA) is the core component of PEM fuel cell and consists of membrane with the gas-diffusion layers including the catalyst attached to each side. It is influenced by varying local conditions of temperature and humidity. Figure 2 shows the distribution of the temperature inside the MEA during the cell operating at base case condition. In general, the temperature at the cathode side is higher than at the anode side, due to the reversible and irreversible entropy production.

Naturally, the maximum temperature occurs, where the electrochemical activity is the highest, which is near the cathode side inlet area. The maximum temperature is more than 7 K above the gas inlet temperature and it occurs inside the cathode catalyst layer, implying that major heat generation takes place in this region.

Due to the varying local conditions of temperature and humidity across the MEA, the hygro and thermal stresses are introduced. Figure 3 shows von Mises stress distribution (contour plots) and deformation shape (scale enlarged 200 times) across the MEA on the y-z plane at x=10 mm. The figure illustrates the effect of stresses on the MEA. Because of the different thermal expansion and swelling coefficients between gas diffusion layers and membrane materials with non-uniform temperature distributions in the cell during operation, hygro-thermal stresses and deformation are introduced. The non-uniform distribution of stress, caused by the temperature gradient in the MEA, induces localized bending stresses, which can contribute to delaminating between the membrane and the GDLs.

Table 2. Electrode and membrane parameters for base case operating conditions

Parameter	Symbol	Value	Unit
Electrode porosity	ε	0.4	-
Electrode electronic conductivity	λ_e	100	S/m
Membrane ionic conductivity (Nafion [®] 117)	λ_m	17.1223	S/m
Transfer coefficient, anode side	α_a	0.5	-
Transfer coefficient, cathode side	α_c	1	-
Cathode reference exchange current density	$i_{o,c}^{ref}$	1.8081e-3	A/m^2
Anode reference exchange current density	$i_{o,a}^{ref}$	2465.598	A/m^2
Electrode thermal conductivity	k_{eff}	1.3	$W/m.K$
Membrane thermal conductivity	k_{mem}	0.455	$W/m.K$
Electrode hydraulic permeability	kp	1.76e-11	m^2
Entropy change of cathode side reaction	ΔS	-326.36	$J/mole.K$
Heat transfer coefficient between solid and gas phase	β	4e6	W/m^3
Protonic diffusion coefficient	D_{H^+}	4.5e-9	m^2/s
Fixed-charge concentration	c_f	1200	$mole/m^3$
Fixed-site charge	z_f	-1	-
Electro-osmotic drag coefficient	n_d	2.5	-
Electrode Poisson's ratio	\mathfrak{S}_{GDL}	0.25	-
Membrane Poisson's ratio	\mathfrak{S}_{mem}	0.25	-
Electrode thermal expansion	\wp_{GDL}	-0.8e-6	$1/K$
Membrane thermal expansion	\wp_{mem}	123e-6	$1/K$
Electrode Young's modulus	Ψ_{GDL}	1e10	Pa
Membrane Young's modulus	Ψ_{mem}	249e6	Pa
Electrode density	ρ_{GDL}	400	kg/m^3
Membrane density	ρ_{mem}	2000	kg/m^3
Membrane humidity swelling-expansion tensor	$\tilde{\lambda}_{mem}$	23e-4	$1/\%$

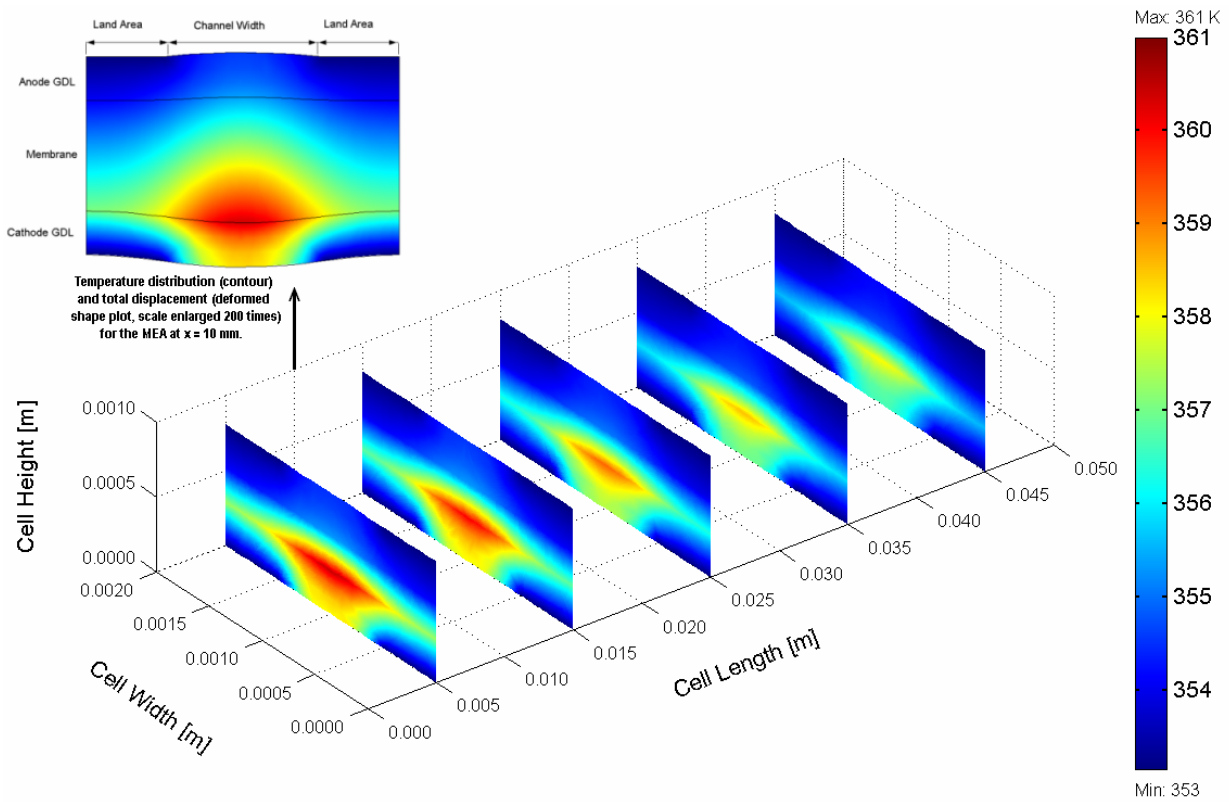


Figure 2. Temperature distribution inside the MEA (Base case conditions)

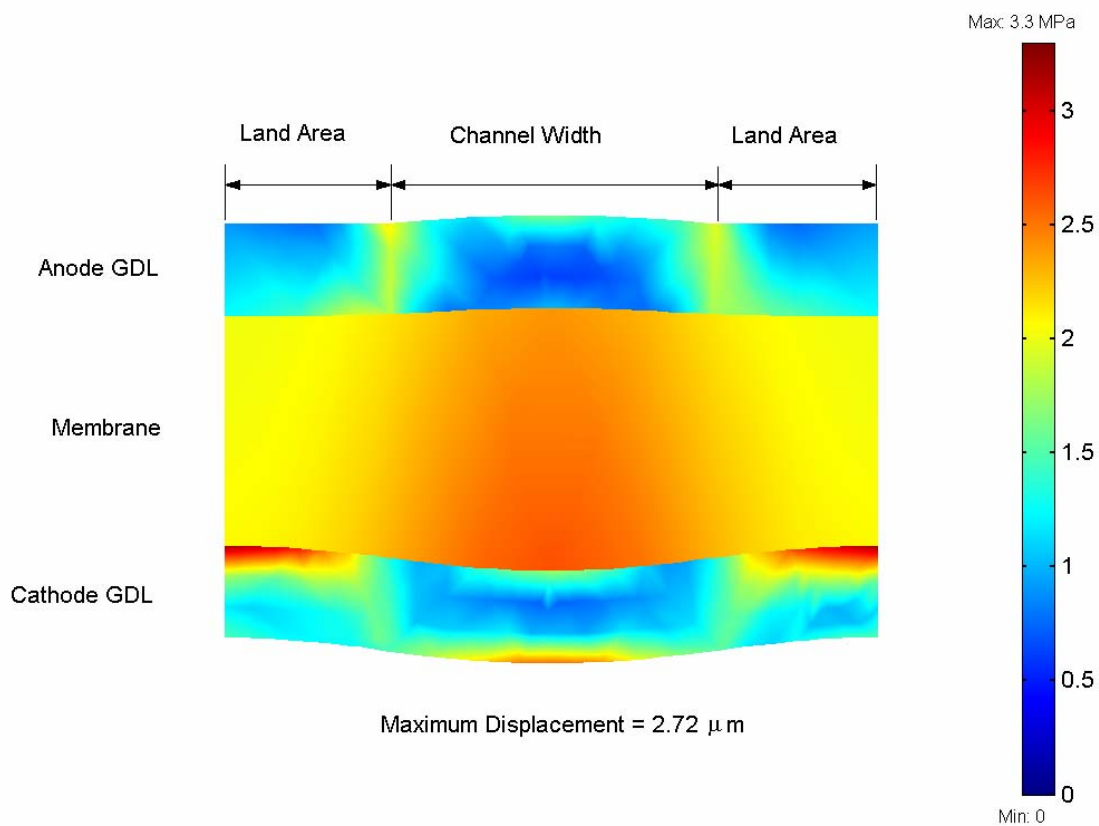


Figure 3. Mises stress distribution (contour) and total displacement (deformed shape plot, X200) in the MEA at base case conditions

3.2 Optimal design to generate maximum power

The material parameters, cell design, and cell operating conditions that give optimal performance depend on the application area. Stationary, portable, and transportation applications all have different requirements, operate in different environments, and the available fuel and oxidant conditions vary greatly. A PEM fuel cell used in a stationary application could operate from fully humidified fuel with high operating temperature and benefit from a compressor to increase air pressure, which increases the cell's power output. In contrast, a fuel cell in portable applications such as laptop PC or cell phone would most likely operate with air at atmospheric conditions. Furthermore, the amount of water available for fuel and air humidification in a portable fuel cell might be limited. Other requirements vary by application. For example, fuel cell weight is much more critical in mobile appliances, and it limits the choice of materials for manufacturing. In order to determine the optimum cell performance, the cell power at various operating conditions is compared at constant nominal current density.

The performance characteristics of the fuel cell based on a certain parameter can be obtained by varying that parameter while keeping all other parameters constant (at base case conditions). Results with different operating conditions for the cell operates at nominal current density of 1.2 A/cm^2 are presented in Figure 4. In the following discussion only the parameter investigated is changed, all other parameters are at the base case conditions as outlined in Table 1 and Table 2.

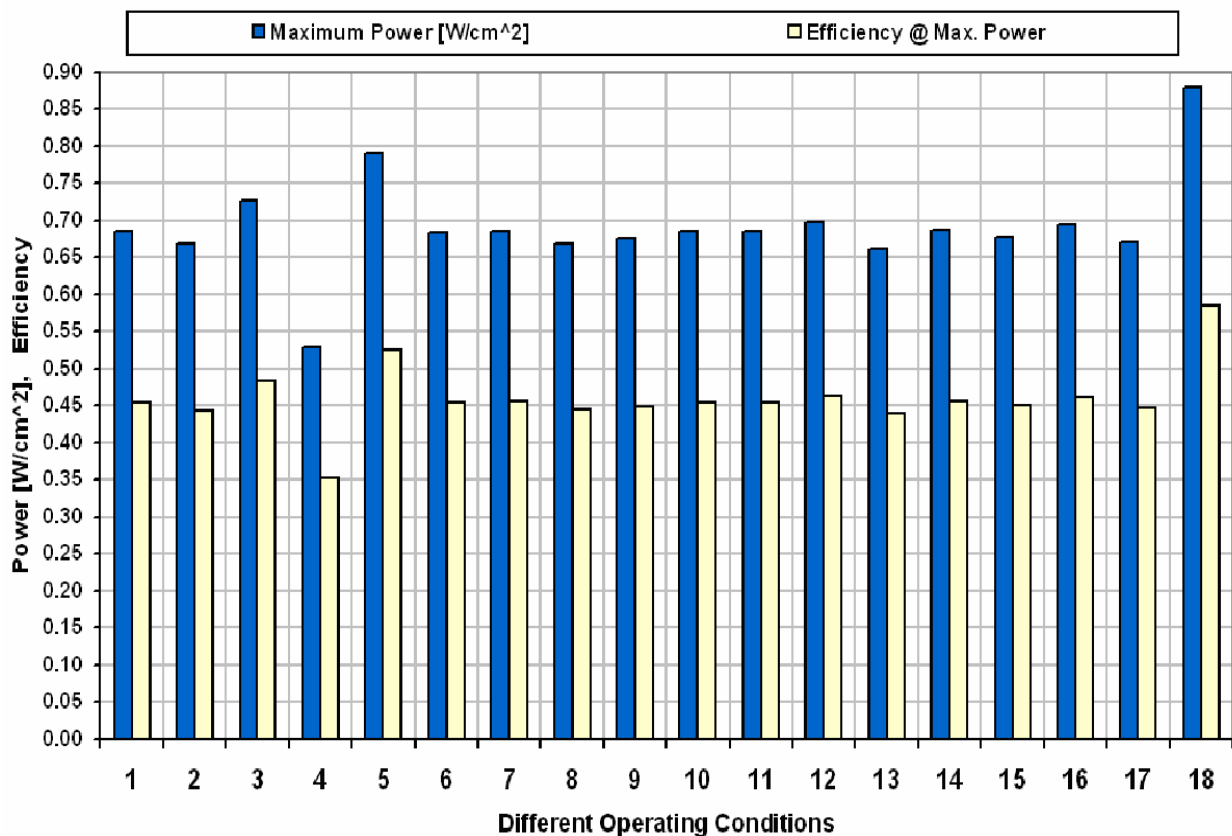


Figure 4. Cell power with corresponding efficiency for different operating conditions.

Key:

- | | |
|--------------------------------------|----------------------------------------------|
| 1- Base case | 10- GDL thermal conductivity = 0.5 W/m.K |
| 2- Cell operating temperature = 60 C | 11- GDL thermal conductivity = 2.9 W/m.K |
| 3- Cell operating temperature = 90 C | 12- Gas channel width = 0.8 mm |
| 4- Cell operating pressure = 1 atm | 13- Gas channel width = 1.2 mm |
| 5- Cell operating pressure = 5 atm | 14- GDL thickness = 0.2 mm |
| 6- Stoichiometric flow ratio = 1.5 | 15- GDL thickness = 0.3 mm |
| 7- Stoichiometric flow ratio = 3 | 16- Membrane thickness = 0.2 mm |
| 8- GDL porosity = 0.3 | 17- Membrane thickness = 0.26 mm |
| 9- GDL porosity = 0.5 | 18- Optimal design to generate maximum power |

In general, the most significant contributor to potential loss for the cell is the cathode catalyst layer. A low permeability and exchange current density combine to demand a significant portion of the reaction free energy. The membrane layer shows sizable potential loss due to low ionic conductivity compared to gas diffusion layer. The loss in the anode catalyst layer is insignificant due to the relatively high permeability of the hydrogen and, more importantly, because the anode reaction is orders of magnitude faster than the cathode for a given activation overpotential.

Higher operating temperature (case 3) will increase the cell power and then the cell efficiency and lower the cost. In addition, the maximum temperature gradient inside the cell will be reduced, but the Mises stresses in membrane will be increased. The activation overpotential decreases with increasing of cell operating temperature. This is because of the exchange current density of the oxygen reduction reaction increases rapidly with temperature due to the enhanced reaction kinetics, which reduces activation losses. A higher temperature leads also to a higher diffusivity of the hydrogen protons in the electrolyte membrane, thereby reducing the membrane resistance and this leads to reducing the potential loss in the membrane. Mass transport loss increases as the cell operating temperature increases due to the reduction of the molar oxygen fraction in the incoming gas streams and, hence, a reduction in the molar oxygen fraction at the catalyst layer.

Operating at a higher pressure (case 5) will increase cell power and efficiency and lower the cost. Also, the maximum temperature gradient inside the cell and the Mises stresses will decrease. However, there will be a higher parasitic power to compress the reactants and the cell stack pressure vessel and piping will have to withstand the greater pressure, which adds extra cost. The activation overpotential decreases with increasing of the cell operating pressure. This is because of the exchange current density of the oxygen reduction reaction increases with increasing of the cell operating pressure due to the enhanced reaction kinetics. To reduce mass transport loss, the cathode is usually run at high pressure. In essence, higher pressures help to force the oxygen and hydrogen into contact with the electrolyte and this leads to reducing the mass transport loss.

Operating at a higher stoichiometric flow ratio (case 7) will increase cell power and efficiency and lower the cost. Also, the maximum temperature gradient inside the cell and the Mises stresses will decrease. However, there is a cost to pay for an increase in the stoichiometric flow ratio. There must be an optimum, where the gain in the cell performance just balances the additional costs of a more powerful blower. This will have to be carefully considered, when designing the fuel cell system.

Operating at lower or higher gas diffusion layer porosities from the base case value (case 8 and 9) will decrease cell power and efficiency, but with higher porosity value the maximum temperature gradient inside the cell and the Mises stresses in membrane will decrease. Higher gas diffusion layer porosity improves the mass transport within the cell and this leads to reducing the mass transport loss (case 9). Another loss mechanism that is important when considering different gas diffusion layer porosities is the contact resistance. Contact resistance occurs at all interfaces inside the fuel cell. The magnitude of the contact resistance depends on various parameters such as the surface material and treatment and the applied stack pressure. The electrode porosity has a negative effect on electron conduction, since the solid matrix of the gas diffusion layer provide the pathways for electron transport, the higher volume porosity increases resistance to electron transport in the gas diffusion layers.

Operating at a higher gas diffusion layer thermal conductivity (case 11) will decrease the maximum temperature gradient inside the cell and this leads to reducing the Mises stresses inside the membrane. Therefore, a gas diffusion layer material having higher thermal conductivity is strongly recommended for fuel cell designed to operate with high power. The cell power and efficiency remains constant for both case of higher and lower values of thermal conductivity.

Operating at a narrow gas flow channel (case 12) will increase cell power and efficiency and lower the cost. In addition, the maximum temperature gradient inside the cell and the Mises stresses in membrane will decrease. However, the pressure drop inside the cell will increase with a narrow gas flow channel. A reduced width of the land area increases the contact resistance between the bipolar plates and the gas diffusion electrodes (case 13). Since this is an ohmic loss, it is directly correlated to the land area width.

Operating with a thinner gas diffusion layer (case 14) will slightly increase cell power and efficiency and lower the cost. However, the maximum temperature gradient inside the cell and the Mises stresses in membrane will increase. The effect of gas diffusion layer thickness on the fuel cell performance is mostly on the mass transport, as the ohmic losses of the electrons inside the gas diffusion layer are relatively small due to the high conductivity of the carbon fiber paper. A thinner gas diffusion layer increases the mass transport through it, and this leads to reduction the mass transport loss.

Operating with a thinner membrane (case 16) will increase cell power and efficiency and lower the cost. In addition, the maximum temperature gradient inside the cell and the Mises stresses in the membrane will decrease. The effect of membrane thickness on the fuel cell performance is mostly on the resistance of the proton transport across the membrane. The potential loss in the membrane is due to resistance to proton transport across the membrane from anode catalyst layer to cathode catalyst layer. Therefore, a reduction in the membrane thickness means that the path travelled by the protons will be decreased; thereby reducing the membrane resistance and this leads to reducing the potential loss in the membrane, which in turn leads to less heat generation in the membrane.

To generate maximum power, the results show that the cell must be operate at higher cell operating temperature, higher cell operating pressure, higher stoichiometric flow ratio, and must have higher GDL porosity, higher GDL thermal conductivity, narrower gases channels, and thinner membrane. The parameters that generate maximum power are presented in Table 3. These parameters have been used in the CFD model to predict the performance, stresses, displacement, and the degree of deformation in the cell for the optimal conditions to generate maximum power (case 18). Figure 5 shows the distribution of the temperature inside the MEA during the cell operating to generate maximum power (the operating conditions are listed in Table 3). The result shows that the temperature increase for the case of optimum design to generate maximum power is less than for the base case operating conditions, only 3 K, and this leads to reducing the total displacement and the degree of the deformation inside the MEA.

Figure 6 shows von Mises stress distribution (contour plots) and deformation shape (scale enlarged 200 times) for MEA on the y-z plane at x=10 mm for optimal operating conditions of maximum power (Table 3). The figure illustrates the effect of stresses on the MEA. The results show that the maximum displacement is 2.6 micro m. This value is less than the displacement that occurs in the base case operating conditions due to the lower temperature gradient in optimum case. The figure is also shows that the Miss stress in the membrane in optimum design case is higher than in the membrane of the base case operating conditions. This is due to operating at a higher cell temperature (90 C).

Table 3. Optimal parameters for optimum design to generate maximum power

Parameter	Value
Cell operating temperature	90 C
Cell operating pressure	5 atm
Stoichiometric flow ratio	3
Gas channel width	0.8 mm
GDL porosity	0.4
GDL thickness	0.3 mm
GDL thermal conductivity	2.9 W/m.K
Membrane thickness	0.2 mm
<ul style="list-style-type: none"> All other parameters keeping constant at base case conditions. (Table 1 and 2) 	

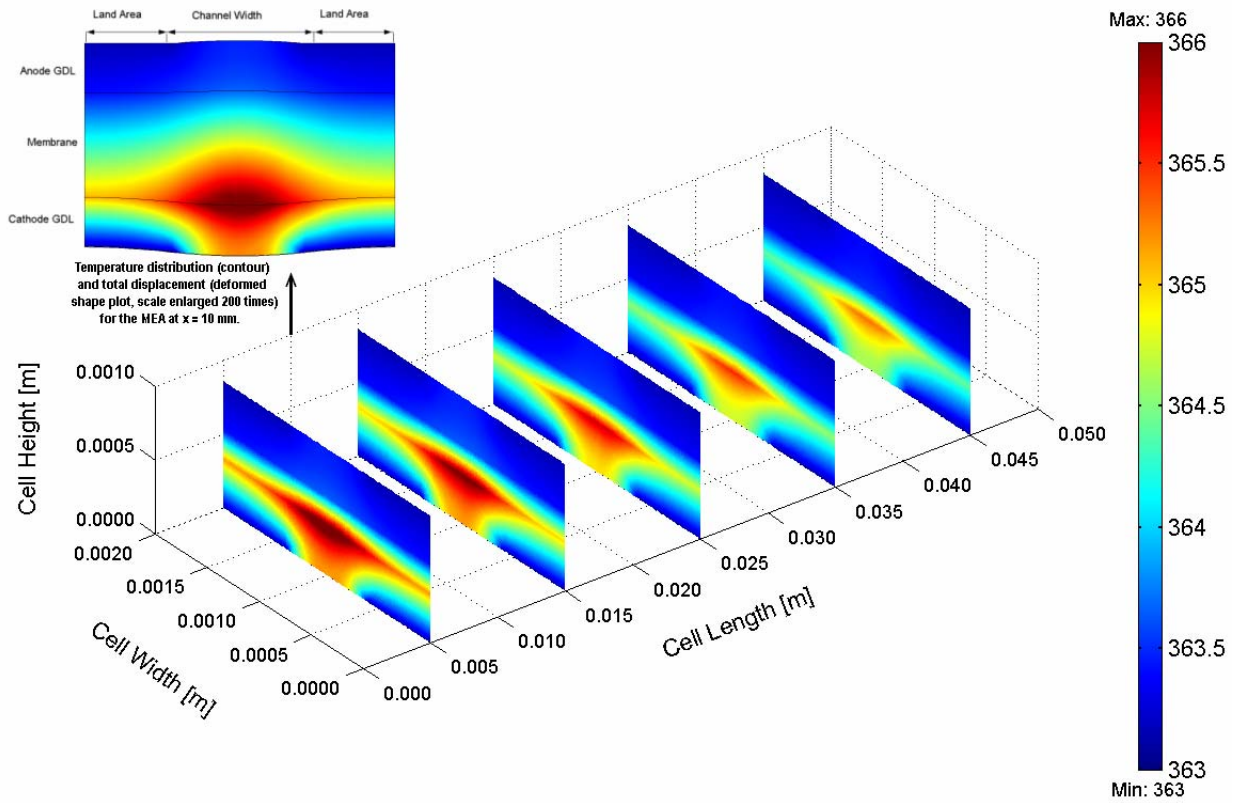


Figure 5. Temperature distribution inside the MEA (Optimal design to generate maximum power)

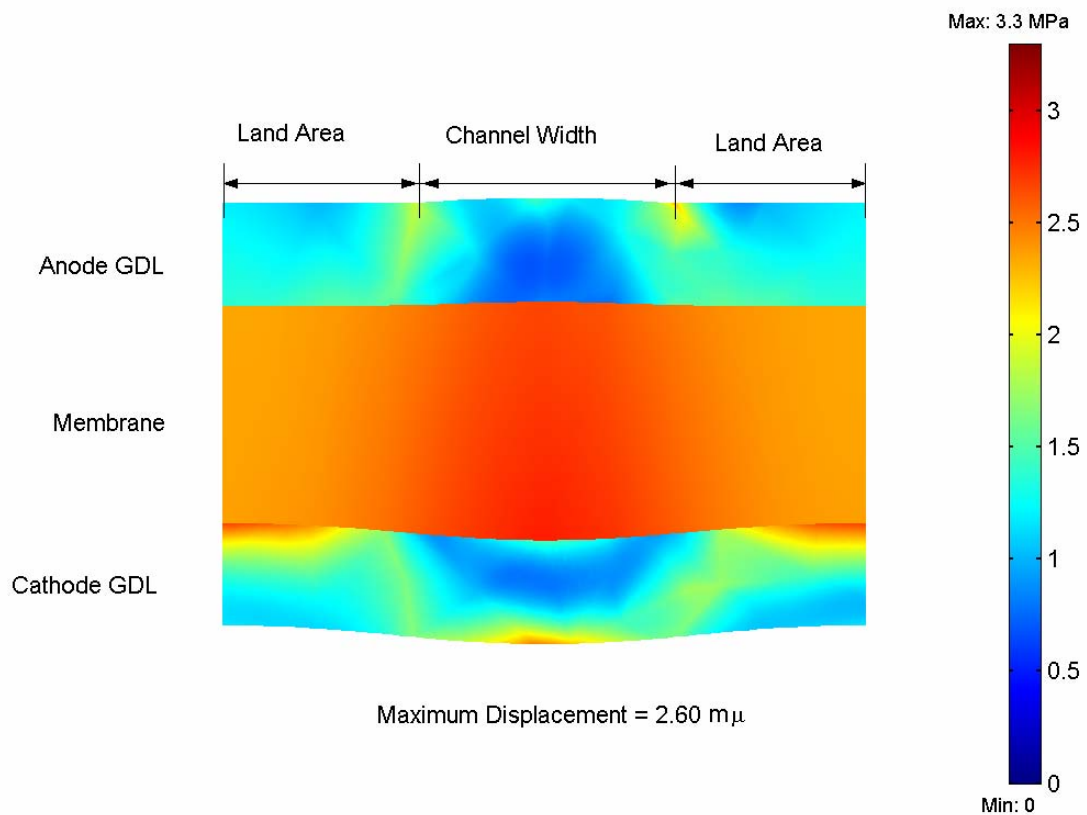


Figure 6. Mises stress distribution (contour) and total displacement (deformed shape plot, X200) in the MEA for optimum design to generate maximum power (the operating conditions are listed in Table 3)

4. Conclusion

A full three-dimensional, multi-phase computational fluid dynamics model of a PEM fuel cell has been developed. The parametric study using this model has been performed and discussed in detail. The study quantifies and analyses the impact of operating, design, and material parameters on fuel cell performance and get an optimal design for PEM fuel cells to generate maximum power. The analysis helped identifying critical parameters and shed insight into the physical mechanisms leading to a fuel cell performance under various operating conditions. To generate maximum power, the results show that the cell must be operate at higher cell operating temperature, higher cell operating pressure, higher stoichiometric flow ratio, and must have higher GDL porosity, higher GDL thermal conductivity, narrower gases channels, and thinner membrane. At these optimum conditions, the result shows that the total displacement and the degree of the deformation inside the MEA were decreased. However, the Miss stress in the membrane was increased due to higher cell operating temperature. In conclusion, the development of physically representative models that allow reliable simulation of the processes under realistic conditions is essential to the development and optimization of fuel cells, improve long-term performance and lifetime, the introduction of cheaper materials and fabrication techniques, and the design and development of novel architectures.

References

- [1] Siegel C. Review of computational heat and mass transfer modeling in polymer-electrolyte-membrane (PEM) fuel cells. *Energy*, 2008; 33, 1331-1352.
- [2] Maher A.R. Sadiq Al-Baghdadi. Modeling optimizes PEM fuel cell durability using three-dimensional multi-phase computational fluid dynamics model. *International Journal of Energy and Environment IJEE*, 2010; 1(3), 375-398.
- [3] Maher A.R. Sadiq Al-Baghdadi. Novel design of a compacted micro-structured air-breathing PEM fuel cell as a power source for mobile phones. *International Journal of Energy and Environment IJEE*, 2010; 1(4), 555-572.
- [4] Maher A.R. Sadiq Al-Baghdadi. A CFD study of hygro-thermal stresses distribution in tubular-shaped ambient air-breathing PEM micro fuel cell during regular cell operation. *International Journal of Energy and Environment IJEE*, 2010; 1(2), 183-198.
- [5] Chun-Hua Min. Performance of a proton exchange membrane fuel cell with a stepped flow field design. *Journal of Power Sources*, 2009, 186, 370-376.
- [6] Jeon D.H., Greenway S., Shimpalee S., Van Zee J.W. The effect of serpentine flow-field designs on PEM fuel cell performance. *Int. J. Hydrogen Energy*, 2008, 33, 1052-1066.
- [7] Cindrell L., Kannana A.M., Lina JF., Saminathana K., Hoc Y., Lind CW., Wertze J. Gas diffusion layer for proton exchange membrane fuel cells-A review. *J. Power Sour* 2009, 194, 146-160.
- [8] F. Brèque, J. Ramousse, Y. Dubé, K. Agbossou, P. Adzakpa. Sensibility study of flooding and drying issues to the operating conditions in PEM Fuel Cells. *International Journal of Energy and Environment IJEE*, 2010; 1(1), 1-20.
- [9] Maher A.R. Sadiq Al-Baghdadi. Mechanical behaviour of PEM fuel cell catalyst layers during regular cell operation. *International Journal of Energy and Environment*, 2010; 1(6), 927-936.
- [10] Tang, Y.; Kusoglu, A.; Karlsson, A.M.; Santare, M.H.; Cleghorn, S.; Johnson, W.B. Mechanical properties of a reinforced composite polymer electrolyte membrane and its simulated performance in PEM fuel cells. *J. Power Sources*, 2008; 175(2): 817-825.
- [11] Bograchev D., Gueguen M., Grandidier J-C., Martemianov S. Stress and plastic deformation of MEA in fuel cells stresses generated during cell assembly. *J. Power Sour*, 2008; 180(2): 393-401.